

## Entrapment of Immature Amyloid Protofilaments in the Hydrophobic Domain of Schizophyllan

Mina Sakuragi, Yoichi Takeda, Naohiko Shimada, and Kazuo Sakurai (✉)

Department of Chemical Processes & Environments and Department of Chemistry,  
The University of Kitakyushu, 1-1 Hibikino, Wakamatu-ku, Kitakyushu, Fukuoka 808-0135,  
Japan

E-mail: sakurai@env.kitakyu-u.ac.jp; Fax: +81-93-695-3390

Received: 18 December 2007 / Revised version: 4 March 2008 / Accepted: 5 March 2008  
Published online: 29 March 2008 – © Springer-Verlag 2008

### Summary

$\beta$ -1,3-glucan schizophyllan (SPG) is known to adopt a triple helical structure in nature and a random coil conformation in alkaline solutions which forms a hydrophobic domain when its random coil is renatured. This paper presents the complexation of amyloid with SPG, presumably owing to hydrophobic interactions between the  $\beta$ -sheets and the SPG hydrophobic domain. Circular dichroism (CD) showed that complex had a negative band at 225nm, indicating the presence of the stacked  $\beta$ -sheets. However, wide angle X-ray scattering (WAXS) showed no clear inter  $\beta$ -sheet diffractions that are generally observed at 1.0 nm in matured amyloid. Combining WAXS and CD, it can be concluded that lysozyme in complex has  $\beta$ -sheets but the  $\beta$ -sheets are not well stacked to give diffraction. Small angle X-ray scattering (SAXS) profile from complex can be reproduced using a combination of the cross-sectional Guinier and Debye-Bueche functions.

### Introduction

Several diseases such as Alzheimer's are related to a particular self-assembled form of misfolded-proteins, called amyloid fibrils.[1] Amyloid fibrils are characterized by their straight and unbranched fibrils (with a diameter of about 10 nm) predominantly composed of multiple protofilaments. These fibrils typically show pathognomonic green birefringence in polarized light after staining with Congo red and X-ray diffraction patterns from amyloid fibrils show 0.47 nm meridional and 1.0 nm equatorial reflections, indicating that the  $\beta$ -strands are perpendicular to the fiber axis and the  $\beta$ -sheets are parallel to the fiber axis.[2] This characteristic structure is called "cross- $\beta$ -conformation" and is the common composition of amyloid protofilaments and mature amyloid fibril typically consists of several protofilaments.[3, 4]

There seems to be no peptide-sequential or three-dimensional macrostructure homology in the amyloid precursor proteins.[1, 3] It seems that the key step in amyloid fibril growth is formation of a  $\beta$ -sheet with subsequent intermolecular aggregation between  $\beta$ -sheets and adoption of this cross- $\beta$ -conformation.[5, 6] Presumably, hydrophobic interactions between  $\beta$ -sheets are responsible for the

formation and growth of the amyloid fibril. There have been several suggestive studies for this, some of whom have tried to control the amyloid fibril formation within the hydrophobic domain of micelles or on the hydrophobic surface of Teflon.[7, 8]

Hen egg lysozyme (Lys) can be precipitated from 90 % ethanol as an amyloid protofilament on addition of a saline solution (10mM).[5] Neutron and small-angle X-ray scattering (SAXS) measurements have showed that Lys can take four distinct structures: monomer, dimer, amyloid protofilament and amyloid fibril depending on the Lys, water and ethanol concentrations.[6] Scattering measurements revealed that these protofilaments have a cross-sectional radius of gyration ( $R_{cg}$ ) of 2.4 nm; only a small increment was observed compared with that of the monomer size (*c.a.* 1.7 nm). Circular dichroism (CD) measurements have shown that the large changes in the secondary structures of Lys occur during the dimer formation. The Lys amyloid protofilaments can be reversibly returned (renatured) to the parent monomer by simple solvation in neutral aqueous solution. Since the physicochemical properties of Lys have been extensively studied previously, Lys is a suitable model for study of the mechanism of amyloid protofilament formation. In fact, most of the above-mentioned studies have used Lys for this reason.

Sakurai and Shinkai have reported that natural polysaccharide schizophyllan (SPG, see Figure 1A for chemical structure) can form complexes with polynucleotides, [9, 10] carbon nanotubes,[11, 12] and some hydrophobic polymers.[13] SPG consists of a  $\beta$ -(1 $\rightarrow$ 3)-D-glucan main chain with one  $\beta$ -(1 $\rightarrow$ 6)-D-glycosyl side chain linked to the main chain at every three glucose residues. In nature, SPG adopts a triple helix structure (t-SPG), which can be denatured to the three composite coils on solvation in dimethyl sulfoxide (DMSO) or alkaline solutions at pH > 13. They showed that the major driving force behind the complexing ability of SPG is the combination of hydrophobic and hydrogen-bonding interactions. This suggests that renatured SPG can provide hydrophobic domains. Indeed, Kasuga et al[14] showed that SPG interferes with folding process of ferricytochrome c during its renaturation process. This demonstrates that the hydrophobic domain of SPG can interact with the hydrophobic moiety in proteins. This paper presents the first evidence for a further novel interaction between SPG and denatured Lys.

## Experimental

### *Materials*

Hen egg-white lysozyme (Lys) (L6876) was purchased from Sigma Chemical Co. and used without further purification. Lys concentrations were determined using an extinction coefficient (at 280 nm) of 2.63.[1] SPG triple helix (t-SPG) was kindly supplied by Mitsui Sugar Co., Ltd. (Japan). The weight-average molecular weight and the number of repeating units were found to be  $1.5 \times 10^5$  (150K) and 231 respectively. Thioflavin and Congo Red were purchased from Sigma Chemical Co. All other reagents were purchased from either Fisher Scientific or Sigma.

### *Sample Preparation*

A-Lys solution of 7 mg/mL containing 90% ethanol and 10mM NaCl was incubated at 25 °C for three days to allow for amyloid protofilament precipitation (A-Lys). This is

the standard protocol for amyloid protofilament formation from Lys.[5] The obtained A-Lys exhibited the Congo Red birefringence and the Thioflavin fluorescence. The renatured Lys (Rn-Lys) was obtained by dissolving A-Lys into a Tris buffer at pH = 7.7. t-SPG was dissolved in an NaOH solution (pH = 13.5) to denature the helix to the random coil (s-SPG). The s-SPG/NaOH solution was added to a large amount of ethanol to induce precipitation. Since ethanol is a poor solvent for both s-SPG and t-SPG, the obtained SPG precipitate mainly consisted of s-SPG. This is because this procedure was too rapid to retrieve t-SPG from s-SPG. The renatured SPG (Rn-SPG) was obtained by dissolving the SPG precipitate into a 10mM Tris buffer at pH =7.7. To obtain a complex, A-Lys (7 mg,  $4.90 \times 10^{-7}$  mol) and the SPG precipitate (7 mg,  $4.32 \times 10^{-5}$  mol in glucose,  $M_w = 150K$ ) were mixed and stood in an ultrasound bath with a HONDA, Ultrasonic Multi Cleaner, W-113, 28 kHz for 15 min, then again mixed vigorously in a mortar for about one minute. The mixture did not dissolve after 7 mL of 10mM Tris buffer was added (we confirmed that pH was maintained at 7.8 after addition of the buffer). We denoted this precipitate dispersed solution S/L (molar ratio of Lys to SPG was 1 : 0.1). A second solution, made with the same procedure, using 3.5 mg of SPG, this solution was named 0.5S/L (a molar ratio of Lys to SPG was 1 : 0.05). We confirmed that there was no precipitate observed in the case that we mixed Rn-SPG and Rn-Lys solutions, followed by they were dissolved in 10mM Tris buffer at pH =7.7, individually.

#### *Small-Angle X-ray Scattering (SAXS)*

The SAXS intensities ( $I$ ) were measured as a function of the magnitude of the scattering vector ( $q$ ) at BL-40B2 (Structural Biology II Beamline) of the synchrotron radiation facility SPring-8, Hyogo, Japan. The exposure time was 300 seconds, the wavelength is 0.10 nm and the camera length was 1.5 m, 1.0 m, or 3.1 m. The samples were loaded into a quartz cell (Mark-Röhrchen) with 2 mm diameter and the protein concentration was fixed at 7 mg/mL.

The SAXS profile from Lys was fitted using a rotational ellipsoid model[15] given by

$$I(q) \propto \int_0^{\pi/2} \Phi^2 \left[ qR(\sin^2 \alpha + \nu^2 \cos^2 \alpha)^{1/2} \right] \sin \alpha d\alpha \quad (1)$$

$$\Phi(x) = \frac{\sin x - x \cos x}{x^3} \quad (2)$$

where the semi-axes are  $R$ ,  $R$ , and  $\nu R$ . The radius of gyration ( $R_g$ ) is related to  $R$  by  $R_g = \{(2+\nu^2)R^2/5\}^{1/2}$ . The SAXS profile from t-SPG was fitted using a rod model[16] given by

$$I(q) \propto \frac{1}{q} \left[ \frac{J_1(qR_c)}{qR_c} \right]^2 \quad (3)$$

where  $J_1(x)$  is the first order Bessel function, the radius of the cylinder is  $R_c$  and the cross-sectional radius of gyration ( $R_{cg}$ ) determined from  $\ln qI(q)$  vs.  $q^2$  plot is related to  $R_c$  by  $R_{cg} = R_c / \sqrt{2}$ . The asymptotic scattering at large  $q$  from rod or rod-like scatters can be expressed by

$$I(q) = \frac{1}{q} \exp\left(-\frac{1}{2} R_{cg}^2 q^2\right) \quad (4)$$

SAXS from aggregate solutions such as amyloid protofilament dispersed in ethanol were fitted by a sum of the two contributions from the corresponding particle scattering  $I_{sol}(q)$  and excess scattering  $I_{ex}(q)$ ;[17]

$$I(q) = I_{sol}(q) + I_{ex}(q) \quad (5)$$

For networks,  $I_{sol}(q)$  can be given by the Lorentz (Ornstein-Zernike, denoted by OZ) function;

$$I_{sol}(q) \propto \frac{1}{1 + \xi^2 q^2} \quad (6)$$

where  $\xi$  (thermal correlation length) can be related to the mesh size of the network (blob size). For  $I_{ex}(q)$ , since the aggregate-dispersed solution can be considered a two-phase system, consisting of solvents and precipitant, we used the Debye-Bueche (DB) function given by;

$$I_{ex}(q) \propto \frac{1}{(1 + \beta^2 q^2)^2} \quad (7)$$

Here, the correlation length,  $\beta$ , represents the long-range heterogeneity of two-phase systems.

### *Wide-Angle X-ray Scattering (WAXS) and Circular Dichroism (CD)*

The precipitant of A-Lys or S/L was dried under vacuum for 24 h. WAXS for these samples were performed on a Rigaku XRD-DSC-II with a slit of 0.15 mm, at a scanning speed of 0.02°/ min from  $2\theta = 2$  to  $30^\circ$  at the Instrumental center of The University of Kitakyushu. Circular dichroism (CD) spectra were recorded using a Jasco 710 CD Spectrophotometer.

## **Results and Discussion**

### *Precipitant formation from S/L mixture*

Lys is known to increase in helical content in ethanol and exists as an amyloid protofilament in 90% ethanol and 10 mM NaCl solution.[5] We treated Lys in such a manner and obtained a white precipitate (denoted by A-Lys) that showed the characteristics of amyloid protofilaments when treated with both Thioflavin and Congo Red. When this precipitant was added to water (pH = 7.7, 10mM Tris buffer) under vigorously mixing, it dissolved completely and a homogenous solution was obtained (Figure 1C), confirming that the amyloid protofilament had become renatured to the water-soluble Lys (Rn-Lys). The SPG precipitant was obtained by adding an s-SPG solution (pH = 13.5) to a large volume of ethanol. When this SPG precipitant was added to water (pH = 7.7, 10mM Tris buffer) it also dissolved to give a Rn-SPG solution (Figure 1C). When we mixed these Rn-SPG and Rn-Lys solutions, there was no precipitant observed. In contrast, when we mixed A-Lys and the SPG

precipitant initially in a mortar, and the mixture was added to water (10mM Tris buffer), the mixture did not dissolve as presented in Figure 1C. This result suggests that mixing the two precipitates in a mortar (i.e., before adding water) caused interactions between A-Lys and SPG. When we treated dextran and amylose in the same manner as presented in Figure 1B (including NaOH treatment), we did not obtain large amounts of precipitate (such as in Figure 1C) although we observed some turbidity after added water to these mixtures.

The hydroxyl groups of SPG become fully deprotonated at a pH greater than 13.5 and should be re-protonated again when they are turned back into natural water or a buffer.[18] However, it is thought that some of these hydroxide anions may not re-protonate when we made SPG precipitate (see Figure 1B) by adding a large amount of ethanol to the s-SPG solution. The SPG precipitant was then washed with an ethanol/HCl solution. This washed (re-protonated again) SPG precipitant was mixed with A-Lys in a mortar in the same way and then the buffer solution was added. In this case, we observed a considerable decrease in the volume of the S/L complex. This seems to imply that these deprotonated hydroxyl groups play an important role in the interaction between SPG and A-Lys.

It is not likely that the complex made from single stranded polysaccharide chains and amyloid fibrils. We presume that hydrophobic interactions between the  $\beta$ -sheets and the SPG hydrophobic domain are the major driving force and these hydrophobic domain can emerge during the re-folding of both SPG and Lys. Once the hydrophobic part of SPG and Lys meet and bind with each other. In this sense, the complexation is not stoichiometric reaction and dynamical factors may be involved, we supposed that more quantitative characterization such as determined the stoichiometric ratio is a rather challenging task. The above experiment indicates that in order to maintain amyloid form after added SPG/buffer, we need at least 0.5S/L, which means one Lys molecule needs 0.05 SPG polymer chain (i.e., 44 glucose residues).

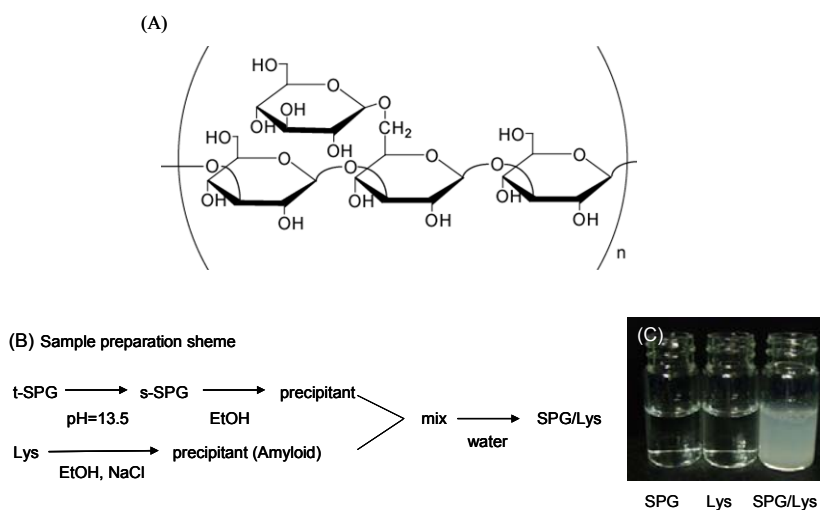


**Figure 1.** (A) Chemical structure of SPG (schizophyllan), (B) Sample preparation scheme of a complex made from SPG and Lys (S/L), and (C) Comparison of solution appearance between renatured SPG (Rn-SPG), renatured Lys (Rn-Lys), and S/L.

One may think that mixing in the mortar is not the best way and lack of reproducibility. We reached the mortar method based on these following control experiments. When A-Lys was added to SPG aqueous solutions, A-Lys immediately renatured to Rn-Lys and no complex had been formed. This is because intra-molecular reactions (such as renaturation) prevail over inter-molecular reactions (complexation). Whereas, when denatured SPG solutions (such as DMSO or NaOH solutions) were added to amyloid ethanol solutions, SPG was immediately precipitated without forming complex with A-Lys. This is because of poor solubility of SPG in ethanol. Furthermore, when an A-Lys/ethanol solution and Tris buffer were added to a large amount of s-SPG/NaOH solution at the same time, nothing happened. Therefore, we concluded that mixing in the mortar is essential for the complex formation. The use of mortar and similar solid state reactions with us were already reported by other groups.[19]

### SAXS

Figure 2A shows SAXS profiles for W-Lys (lysozyme dissolved to water) and Rn-Lys at the bottom. At  $q > 0.6 \text{ nm}^{-1}$ , the profiles are almost identical. Since this region reflects intramolecular diffractions, these identical profiles imply that Lys undergoes renaturation in which Rn-Lys regains the same shape as W-Lys. The solid line represents the theoretical profiles for a prolate ellipsoid with a rotational axis of 3.5 nm and equatorial radii of 1.45 nm. At  $q > 0.6 \text{ nm}^{-1}$ , experimental data correlates well with this theoretical profile. At  $q < 0.6 \text{ nm}^{-1}$ , the experimental profile of Rn-Lys deviated upward from the theoretical data, while W-Lys showed a downward deviation. The downward deviation may be ascribed to a concentration effect which indicates that the W-Lys molecules are homogeneously dispersed in solutions,[20] presumably, owing to electrostatic repulsion. The upward deviation can be related to a small amount of partial aggregation of Rn-Lys molecules.

The middle profiles in Figure 2A compare t-SPG and Rn-SPG. t-SPG shows the expected power law of  $I(q) \sim q^{-1}$  in the range of  $0.2 \text{ nm}^{-1} < q < 1.0 \text{ nm}^{-1}$ , confirming its rod-like nature (the persistence length was determined to be 200 nm[21]). At  $q > 3 \text{ nm}^{-1}$ , t-SPG shows essentially no deviation from the predicted curve (calculated from Eq 2 and is represented with a solid line), which can be ascribed to the mono-dispersed radius of the rod of t-SPG. The radius of the cylinder was determined to be 0.83 nm. This value is consistent with that of crystallographic data.[22] Rn-SPG also displays a power law for these rods in the same range as t-SPG. This result is consistent with other observations using AFM and TEM that showed a rod-like architecture for renatured SPG. Rn-SPG showed a downward deviation from t-SPG at  $1.0 \text{ nm}^{-1} < q < 3.0 \text{ nm}^{-1}$  and a shallower decrease at  $q = 4.0 - 6.0 \text{ nm}^{-1}$ , indicating a large distribution in the rod radius due to the renaturation process. The slope at  $q > 4.0 \text{ nm}^{-1}$  is approximately -2, which may suggest the presence of a network composed of SPG single chains.

SAXS data for A-Lys is presented at the top of Figure 2A. The slopes of the highest and lowest  $q$  regions are -2.0 and -3.5, respectively. The curve appears to show a stepwise decrease in slope with increasing  $q$ , (although, when carefully examined, it can be found that the slope becomes almost -4 around  $q = 0.2 \text{ nm}^{-1}$ ). The slope in the highest  $q$  region is consistent with the asymptotic behavior of the OZ function given by Eq 5. This means that the scattering in this range is derived from networks made from Lys protofilaments. At  $0.15 \text{ nm}^{-1} < q < 0.2 \text{ nm}^{-1}$ ,  $I(q)$  almost obeys a power law of  $q^{-4}$ , suggesting that there is a sharp interface between the protofilament-network

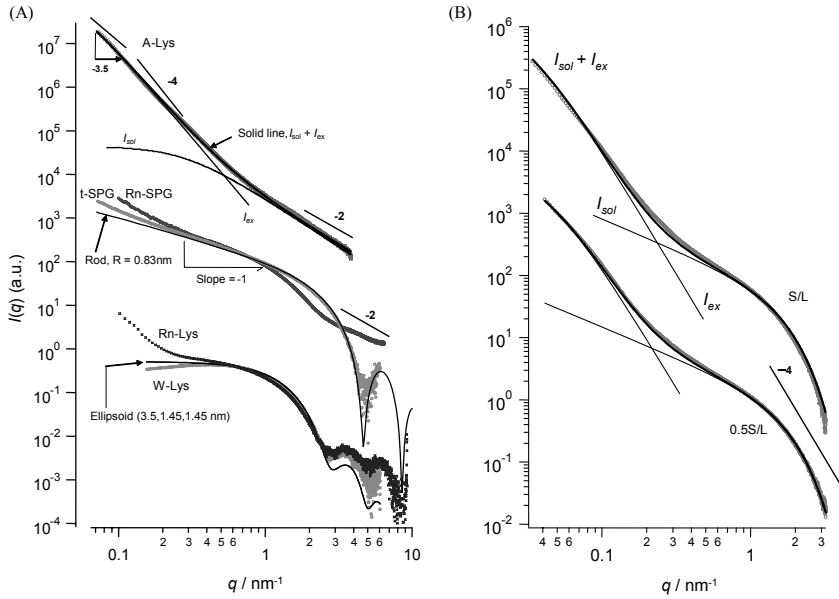


**Figure 2.** (A) Small-angle X-ray scattering profiles from Rn-Lys and W-Lys (bottom), t-SPG and Rn-SPG (middle), and A-Lys (top). The solid lines present the best-fit calculated values from an ellipsoid (Eq 1), and a rod (Eq 2), and Eq 4 using combination of Ornstein-Zernike and Debye-Bueche functions. (B) Small-angle X-ray scattering profiles from S/L and 0.5S/L and the best-fit curves.

Table 1. The best fit parameters

Sample code	$R_g$ or $R_{cg}$ / nm	Model	Best fit parameters
W-Lys	$R_g=3.3$	e	3.5, 1.45, 1.45 nm
Rn-Lys	-	e	3.5, 1.45, 1.46 nm
t-SPG	$R_{cg}=0.59$	r	0.83 nm
Rn-SPG	$R_{cg}=1.01$	r	-
A-Lys	-	DB+OZ	$\beta=30$ nm, $\xi=4$ nm
S/L	-	DB+r	$\beta=37$ nm, $R_{cg}=0.85$ nm
0.5S/L	-	DB+r	$\beta=26$ nm, $R_{cg}=0.81$ nm

e: ellipsoide, r: rod, DB: Debye-Bueche, OZ: Ornstein-Zernicke

domain and the solvent domain. At  $q < 0.1$  nm<sup>-1</sup>, the  $q$  dependence of  $I(q)$  is about  $q^{-3.5}$ , lower than that in the region  $0.15$  nm<sup>-1</sup>  $< q < 0.2$  nm<sup>-1</sup>. These two features may be further considered using the DB equation. We fitted the data points to a combination of the DB and OZ functions. The best fit and individual curves are presented by solid lines (Figure 2A), we obtained  $\beta = 25$ – $35$  nm and  $\xi = 3$ – $10$  nm, respectively. These values suggest that the mesh size of the protofilament is about 3–10 nm and the size of the protofilament domain is about 25–35 nm.

Figure 2B shows SAXS profiles from S/L and 0.5S/L. Both samples show a sharp decrease (greater than -4) at  $2$  nm<sup>-1</sup>  $< q$ , suggesting that the scattering constituent units can be expressed using the cross-sectional Guinier (Eq 3) or normal Guinier (i.e.,  $I(q) \propto \exp(-R_g^2 q^2 / 3)$ ) expression. When we used a combination of Eq 3 and DB, the profiles showed excellent correlation as presented in Figure 2B. The resultant

parameters are listed in Table 1. At  $1\text{-}2\text{ nm}^{-1} < q$ , the  $q$  dependences of S/L and 0.5S/L are similar to that of t-SPG. The  $R_{cg}$  values for S/L and 0.5S/L lie between t-SPG and Rn-SPG. These two facts suggest that the SPG component determines the SAXS at this high  $q$  region. We did not observe a final slope of  $-2$  at low  $q$ , suggesting that there was no network structure in the S/L and 0.5S/L samples. Contrasting the similar  $q$  dependence of t-SPG and S/L, S/L (or 0.5S/L) at low  $q$  values shows a much steeper  $q$ -dependence on  $I$  than that of Rn-SPG and t-SPG. This feature reflects the presence of two phases. Calculated values for  $\beta$  for S/L are of the same order as A-Lys.

### WAXS

Figure 3 compares the WAXS profiles for Lys, A-Lys, S/L, s-SPG. A-Lys has a relatively sharp diffraction at  $0.46\text{ nm}$  and a more diffused one at  $1.0\text{ nm}$ , which are characteristic for amyloid protofilaments. The former corresponds to diffraction between  $\beta$ -strands within the same  $\beta$ -sheet and the latter, between multilayer  $\beta$ -sheets. Generally, in the amyloid fibers,  $\beta$ -strands line perpendicular to the fiber axis and  $\beta$ -sheets line parallel to the fiber axis. Lys has a peak at  $1.0\text{ nm}$  while there is no peak at  $0.46\text{ nm}$ . This peak at  $1.0\text{ nm}$  is ascribed to the intramolecular structure such as  $\alpha$ -helix and  $\beta$ -sheet[23].

S/L has a smaller peak at  $1.0\text{ nm}$  than those of A-Lys and W-Lys. There are two possible assignments for this peak. One is due to the diffraction adjacent  $\beta$ -sheet similar to A-Lys. For this case the weak peak indicates that the stacked layer of  $\beta$ -sheets was not grown sufficiently to give clear diffraction. The other assignment is due to the intramolecular structure similar to W-Lys. The former is more likely because CD in the next section indicated that most  $\alpha$ -helices were eliminated and  $\beta$ -sheet dominated and started stacking. S/L showed a peak at  $0.46\text{ nm}$ , although less sharp than that of A-Lys and thus it might be difficult to distinguish from the peak of SPG. Since neither s-SPG nor Lys has a peak at this position, this S/L peak can be assigned to the inter  $\beta$ -strand diffraction.

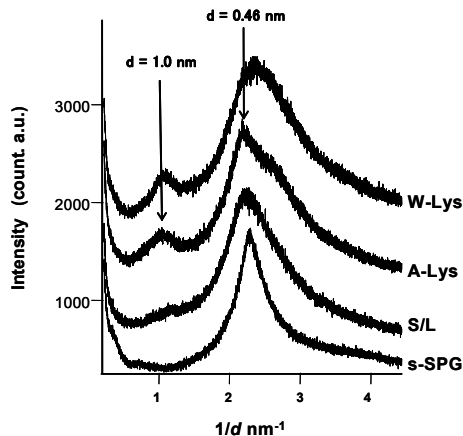


**Figure 3.** Comparison of wide-angle X-ray diffraction patterns among W-Lys, A-Lys, S/L, and s-SPG. The peaks indicated by arrows show diffraction between  $\beta$ -strands within the same  $\beta$ -sheet ( $0.46\text{ nm}$ ) and between adjacent  $\beta$ -sheets ( $1.0\text{ nm}$ ).



## CD

According to previous studies the  $\alpha$ -helix structure of native Lys exhibits two broad negative bands at 208 and 220 nm.[5, 6] Addition of ethanol (up to 85% vol/vol) increases these  $\alpha$ -helix bands at first, but further addition causes to these bands to disappear and a new negative band appear at 215 nm, corresponding to the formation of  $\beta$ -sheets. This  $\beta$ -sheet formation can be further confirmed by appearance of a new sharp positive band at 197 nm. As reported by Yonezawa et al,[6] the transition from  $\alpha$ -helix to  $\beta$ -sheet takes place at the dimer state. Along with the beginning of  $\beta$ -sheet stacking, the 215 band becomes less intense and red-shifts.[7] This change is related to twisting and stacking of the  $\beta$ -sheets and thus can be considered as a precursory phenomenon for the Amyloid fibril formation.

Figure 4 presents the CD spectra for Rn-Lys and A-Lys comparing with those of Lys in 90% ethanol with no salt, and of 90% ethanol with 10mM NaCl (i.e., before incubation to obtain A-Lys). As expected, Rn-Lys and A-Lys show the typical  $\alpha$ -helix and stacked  $\beta$ -sheet bands. As reported, the intense negative band of un-stacked  $\beta$ -sheets around 215 nm changed to a red-shifted weak band around 225 on addition of salt and subsequent incubation. The right spectra compare with A-Lys, S/L, and 2S/L (a mass ratio of Lys to SPG is 1 : 2). S/L and 2S/L show a negative minimum at 225 nm, which mirrored in the CD spectrum of A-Lys. The similarities between the CD spectra of A-Lys and S/L point to the Lys in S/L adopting a similar  $\beta$ -sheet conformation where the  $\beta$ -sheets are stacked in the same manner as the amyloid protofilaments.

After centrifuged an S/L solution to obtain a clear supernatant, we examined whether it contained Rn-Lys. The spectrum could not be assigned to  $\alpha$ -helix, while when Lys was renatured by simply adding A-Lys to water, CD showed a large amount of  $\alpha$ -helix as presented in Figure 4. The fact that the supernatant of S/L solution showed little  $\alpha$ -helix implies that most of Lys are complexed with SPG. When we decreased SPG ratio less than 0.5S/L, the supernatant showed  $\alpha$ -helix CD.

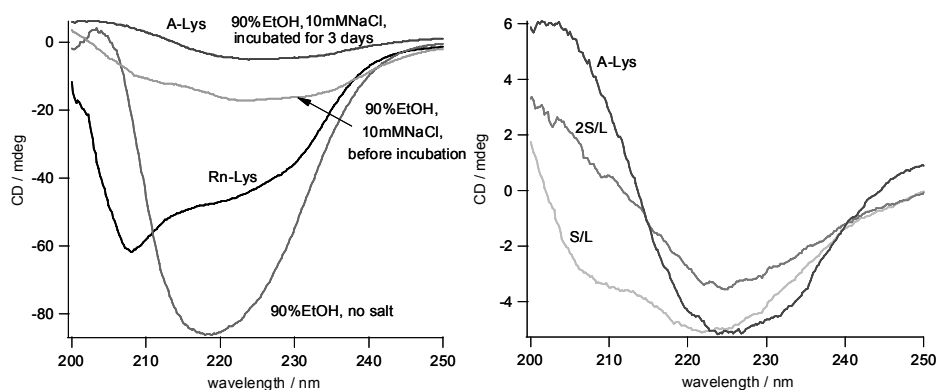


**Figure 4.** Circular dichroism spectra for Lys. The left ones compare three different states:  $\alpha$ -helix rich Rn-Lys, un-stacked  $\beta$ -sheets (90% ethanol, no salt), and stacked  $\beta$ -sheets (A-Lys). The right ones compares S/L and A-Lys. The Lys concentration was 1 mg/mL for all samples.

### *Entrapment of Immature Amyloid Protofilaments*

WAXS did not show a clear  $\beta$ -sheet stacking peak. However, CD showed that S/L has a near-comparable level of  $\beta$ -sheet stacking as that in A-Lys. Since there should be at least ten structural repeats in order to give a perceptible X-ray diffraction, we can conclude that stacking in S/L is immature enough so as not to display WAXS diffraction but still give a CD signal. Therefore, we can postulate that immature amyloid protofilaments become trapped by SPG when A-Lys was mixed with s-SPG and the mixture dispersed in water. The protofilament is renatured if mixed with water alone. The entrapment is likely assisted by the deprotonated hydroxyl groups of SPG that can bind to the cationic groups of Lys. We presume that once misfolded, Lys and/or Lys  $\beta$ -sheets are irreversibly bound to SPG in this way, i.e. they can be easily incorporated into the hydrophobic domain of SPG and the hydrophobic interactions between the  $\beta$ -sheet and the SPG stabilizes the complex.

### **Conclusions**

We presented the complexation of an amyloid protofilament with SPG owing to hydrophobic interactions between the  $\beta$ -sheets and the SPG hydrophobic domain. WAXS showed that this complexed protofilament did not show a clear  $\beta$ -sheet stacking peak. CD indicated the presence of the stacked  $\beta$ -sheets. We propose that stacked  $\beta$ -sheets in the complex are not mature enough to give prominent X-ray diffraction peaks. SAXS suggested that the immature protofilament was entrapped by renatured SPG.

*Acknowledgements.* This work is financially supported by the SORST program of the Japan Science and Technology Agency and Grant-in-Aid for Scientific Research (No. 16350068 and 16655048). SAXS, at SPring-8 BL40B2 (2006A1510).

### **References**

1. Westermark P, Benson MD, Buxbaum JN, Cohen AS, Frangione B, Ikeda S, Masters CL, Merlini G, Saraiva MJ, Sipe JD (2005) Amyloid: toward terminology clarification. Report from the Nomenclature Committee of the International Society of Amyloidosis. *Amyloid* 12:1-4
2. Sunde M, Blake C (1997) The structure of amyloid fibrils by electron microscopy and X-ray diffraction. *Adv Protein Chem* 50:123-159
3. Jimenez JL, Guijarro JI, Orlova E, Zurdo J, Dobson CM, Sunde M, Saibil HR (1999) Cryo-electron microscopy structure of an SH3 amyloid fibril and model of the molecular packing. *Embo J* 18:815-821
4. Petkova AT, Ishii Y, Balbach JJ, Antzutkin ON, Leapman RD, Delaglio F, Tycko R (2002) A structural model for Alzheimer's beta -amyloid fibrils based on experimental constraints from solid state NMR. *Proc Natl Acad Sci U S A* 99:16742-16747
5. Goda S, Takano K, Yamagata Y, Nagata R, Akutsu H, Maki S, Namba K, Yutani K (2000) Amyloid protofilament formation of hen egg lysozyme in highly concentrated ethanol solution. *Protein Sci* 9:369-375
6. Yonezawa Y, Tanaka S, Kubota T, Wakabayashi K, Yutani K, Fujiwara S (2002) An insight into the pathway of the amyloid fibril formation of hen egg white lysozyme obtained from a small-angle X-ray and neutron scattering study. *J Mol Biol* 323:237-251
7. Giacomelli CE, Norde W (2003) Influence of hydrophobic Teflon particles on the structure of amyloid beta-peptide. *Biomacromolecules* 4:1719-1726

8. Marcinowski KJ, Shao H, Clancy EL, Zagorski MG (1998) Solution Structure Model of Residues 1-28 of the Amyloid b-Peptide When Bound to Micelles. *J.Am.Chem.Soc.* 120:11082-11091
9. Sakurai K, Shinkai S (2000) Molecular Recognition of Adenine, Cytosine, and Uracil in a Single-Stranded RNA by a Natural Polysaccharide: Schizophyllan. *J. Am. Chem. Soc* 122:4520-4521
10. Sakurai K, Mizu M, Shinkai S (2001) Polysaccharide--polynucleotide complexes. 2. Complementary polynucleotide mimic behavior of the natural polysaccharide schizophyllan in the macromolecular complex with single-stranded RNA and DNA. *Biomacromolecules* 2:641-650
11. Numata M, Hasegawa T, Fujisawa T, Sakurai K, Shinkai S (2004) Beta-1,3-glucan (schizophyllan) can act as a one-dimensional host for creation of novel poly(aniline) nanofiber structures. *Org Lett* 6:4447-4450
12. Numata M, Asai M, Kaneko K, Bae AH, Hasegawa T, Sakurai K, Shinkai S (2005) Inclusion of cut and as-grown single-walled carbon nanotubes in the helical superstructure of schizophyllan and curdlan (beta-1,3-glucans). *J Am Chem Soc* 127:5875-5884
13. Li C, Numata M, Bae AH, Sakurai K, Shinkai S (2005) Self-assembly of supramolecular chiral insulated molecular wire. *J Am Chem Soc* 127:4548-4549
14. Kasuga M, Shimada N, Takeda Y, Shinkai S, Sakurai K (2006) Encapsulation of Ferricytochrome c into the Nanoparticle Made from a Natural Polysaccharide: Schizophyllan. *Chemistry Letters*, 35(10):1120-1121
15. Martel P, Kim SM, Powell BM (1980) Physical characteristics of human transferrin from small angle neutron scattering. *Biophys J* 31:371-380
16. Terech P, Weiss R (2000) *Molecular Gels*.
17. Shibayama M, Jinnai H, Hashimoto T (2000) *Neutron Scattering*. Academic Press
18. Marchessault RH, Imada K, Bluhm T, Sundararajan PR (1980) Conformation of crystalline type III pneumococcal polysaccharide. *Carbohydr Res* 83:287-302
19. Kihara N, Hinoue K, Takata T (2005) Solid-State End-Capping of Pseudopolyrotaxane Possessing Hydroxy-Terminated Axle to Polyrotaxane and Its Application to the Synthesis of a Functionalized Polyrotaxane Capable of Yielding a Polyrotaxane Network *Macromolecules* 38(2):223-226
20. Stradner A, Cardinaux F, Schurtenberger P (2006) A small-angle scattering study on equilibrium clusters in lysozyme solutions. *J Phys Chem B Condens Matter Surf Interfaces Biophys* 110:21222-21231
21. Kashiwagi Y, Norisuye T, Fujita H (1981) Triple helix of Schizophyllum commune polysaccharide in dilute solution. 4. Light scattering and viscosity in dilute aqueous sodium hydroxide *Macromolecules* 14(5):1220-1225
22. Deslandes Y, Marchessault RH, Sarko A (1980) Triple-Helical Structure of (13)-beta-D-Glucan *Macromolecules* 13:1466-1471
23. Hirai M, Koizumi M, Hayakawa T, Takahashi H, Abe S, Hirai H, Miura K, Inoue K (2004) Hierarchical map of protein unfolding and refolding at thermal equilibrium revealed by wide-angle X-ray scattering. *Biochemistry* 43:9036-9049